Supplementary Information

Iridium Motif Linked Porphyrins for Efficient Light-driven Hydrogen Evolution via Triplet State Stabilization of Porphyrin

Daniel Nnaemaka Tritton,[a]‡ Govardhana Babu Bodedla,[a]‡ Geliang Tang,[b] Jianzhang Zhao,[b] Ken Chak-Shing Kwan,[a] Ken Cham-Fai Leung,[a,*] Wai-Yeung Wong,[a,c,*] and Xunjin Zhu[a,*]

[a]Department of Chemistry, Hong Kong Baptist University, Kowloon Tong, Kowloon, Hong Kong SAR (P. R. China).

[b]School of Chemical Engineering, Dalian University of Technology, Dalian, China

[c]Department of Applied Biology & Chemical Technology, The Hong Kong Polytechnic University, Hong Kong, China; The Hong Kong Polytechnic University Shenzhen Research Institute, Shenzhen, 518057, China

‡ D.N.T and G.B.B contributed equally to this work.

E-mail: cfleung@hkbu.edu.hk; wai-yeung.wong@polyu.edu.hk and xjzhu@hkbu.edu.hk

Experimental Section

Materials and Methods

All the chemicals used in this work were purchased from commercial sources and used as received. Solvents were dried by distilling over suitable dehydrating agents according to the standard procedures. Purification of the compounds was performed by column chromatography with 100-200 mesh silica. ^{1}H and ^{13}C NMR spectra recorded in a Bruker NMR spectrometer operating at 400 and 101 MHz respectively. The chemical shifts were calibrated from the residual peaks observed for the deuterated solvents chloroform ($CDCl_3$) at δ 7.26 ppm for ^{1}H and δ 77.0 ppm for ^{13}C, respectively and acetone ($(CD_3)_2CO$) at δ 2.05 ppm for ^{1}H. High-resolution matrix-assisted laser desorption/ionization time-of-flight

(MALDI-TOF) mass spectra were obtained with a Bruker Autoflex MALDI-TOF mass spectrometer. The optical absorption and emission spectra of the porphyrins were measured for the freshly prepared air equilibrated solutions at room temperature by using UV-Vis spectrophotometer and spectrofluorimeter, respectively. Cyclic voltammetry (CV) was recorded on an electrochemical workstation in acetonitrile (MeCN) solution by using 0.1 M tetrabutylammonium hexafluorophosphate ($TBAPF_6$) as supporting electrolyte. The experiments were performed at room temperature with a conventional three-electrode cell assembly consisting of a platinum wire as auxiliary electrode, a non-aqueous $Ag/AgNO_3$ reference electrode, ferrocene as internal standard and a glassy carbon working electrode.

Relative photoluminescence quantum yields (Φ_{PL})

Relative luminescence quantum yields in the solution state were measured by the optical dilute method reported by Demas and Crosby.[1] A degassed solution of $[Ru(bpy)_3]Cl_2$ in CH_3CN solution (Φ_{lum} = 0.06, excitation wavelength at 436 nm) was used as the reference.[2] The absorbance of the sample and reference solutions was measured by keeping them at 0.1 and the emission of the sample and reference solutions was recorded at 436 nm excitation wavelength. The Φ_{PL} was calculated according to the following equation (Eq. 1):

$$\Phi_F^{sample} = \Phi_F^{ref}\left(\frac{S_{sample}}{S_{ref}}\right)\left(\frac{A_{ref}}{A_{sample}}\right)\left(\frac{n_{sample}{}^2}{n_{ref}{}^2}\right) \quad (1)$$

where A_{ref}, S_{ref}, n_{ref}, *and* A_{sample}, S_{sample}, n_{sample} represent the absorbance at the excited wavelength, integrated area under the photoluminescence curves and the solvent refractive index of the standard and the sample solutions.

Transient absorption measurement

Transient absorption spectra and excited-state lifetimes were obtained using an Edinburgh Instrument LP980KS transient absorption spectrometer equipped with R928P photomultiplier tube and a Tektronix Model TDS-3012C (100 MHz, 1.25 GS s^{-1}) digital oscilloscope. All

solutions for photophysical studies were degassed on a high-vacuum line in a two-compartment cell consisting of a 10-mL Pyrex bulb and a 1-cm path length quartz cuvette and sealed from the atmosphere by a Bibby Rotaflo HP6 Teflon stopper. The solutions were rigorously degassed with no less than four successive freeze-pump-thaw cycles. All absorption data is shown in Table 2.

Preparation of photocatalytic systems

A multichannel photochemical reaction system fixed with OLED white light (PCX50B, 148.5 mW/cm^2) was used as the light source. The photocatalytic hydrogen (H_2) evolution experiments were performed in a quartz vial reactor (20 mL) sealed with a rubber septum, gas-closed system, at ambient temperature and pressure. Initially, the prepared sample (100 μM) was dissolved in a mixture of MeCN/H_2O (2:1 v/v) and triethylamine (TEA) (0.8 M) under constant stirring. Then, cobaloxime (**CoPyCl**) (0.4 mM) co-catalyst was added. The suspension was purged with argon gas for 10 min to ensure anaerobic conditions and then it was placed in a multichannel photochemical reaction system. After 5 hours of irradiation, the released gas (400 μL) was collected by syringe from the headspace of the reactor and was analyzed by gas chromatography (Shimadzu, GC-2014, Japan, with ultrapure Ar as a carrier gas) equipped with a TDX-01(5 Å molecular sieve column) and a thermal conductivity detector (TCD). Eventually, the total content of photocatalytic H_2 evolution was calculated according to the standard curve. Continuous stirring was applied to the whole process to keep the photocatalyst particles in suspension state and to achieve uniform irradiation.

- The apparent quantum efficiency (AQE) was measured under the similar photocatalytic reaction conditions except using 420 nm OLED light. The focused intensity and illuminated area LED light were ca. 68.0 mW/cm^2 and 9.04 cm^2, respectively. AQE was calculated via the following equation:

$$\text{AQE} = \left(\frac{2 \times number\ of\ hydrogen\ molecules}{number\ of\ incident\ photons} \right) \times 100\ \%$$

- The turnover number (TON) was calculated after 1 hour by using the following formula;

$$\text{TON} = \frac{Number\ of\ moles\ of\ hydrogen\ produced\ in\ photocatalytic\ system}{Number\ of\ moles\ of\ photocatalyst}$$

Photoelectrochemical Measurement

To get more insight into the photocatalytic electron transfer mechanism and consequently ηH_2, the transient photocurrent responses (I–t curves) studies were performed using an electrochemical workstation (CHI660C Instruments, China) with Pt wire (counter electrode), a non-aqueous $Ag/AgNO_3$ (reference electrode) and fluorine-doped tin oxide (FTO) glass coated with a porphyrins on the conductive surface (working electrode) upon irradiation of LED monochromatic point lamp (3 W, 420 nm). The light spot effective area on the working electrode was set as 28.26 mm^2. Typically, the working electrode was prepared by dissolving 100 μM of porphyrins in 200 μL of chlorobenzene and then applied on the conductive surface of FTO glass using drop dispense method. 5 mL volume of 0.5 M Na_2SO_4 aqueous solution acted as the electrolyte. The open-circuit voltages were set as the initial bias voltages in the transient photocurrent responses tests. As shown below in Fig S11, the Ir linked porphyrins **MBPyZnP-Ir** and **TBPyZnP-Ir** exhibit a higher photocurrent response than their corresponding analogues **MBPyZnP** and **TBPyZnP** containing no Ir motif. This indicates the efficient photogenerated charge carrier's separation and more electrons generated for the Ir motif linked porphyrins. Especially, **TBPyZnP-Ir** exhibited the highest photocurrent response in the series, further attesting to its higher PHE when it was employed as a photosensitizer. All these results indicate that incorporation of the Ir motif to BPy zinc

porphyrins is beneficial to improve the PHE by enhancing the photogenerated electrons and their transfer from photo excited porphyrins to **CoPyCl** co-catalyst.

Synthesis

The bipyridyl aldehyde intermediate for preparation of the BPy poprhyrins, 4'-methyl-2,2'-bipyridine-4-carbaldehyde was synthesized by a modified procedure to that of Araki *et al.* and characterized by comparing the ^{1}H NMR spectrum of the compound to that found in the literature.[3] The precursor C^N ligand for the iridium dimer, 2-phenyl-5-(trifluorophenyl)-pyridine was synthesized by a modified procedure to that of Wang *et al.* and characterized by comparing the ^{1}H NMR spectrum of the compound to that found in the literature.[4] The cyclometalated iridium dimer intermediate, bis(2-phenyl-5-(trifluorophenyl)-pyridine) iridium (III) dichloro-bridged dimer was synthesized by a modified procedure to that of Chen *et al.* and characterized by comparing the ^{1}H NMR spectrum of the compound to that found in the literature.[5]

MBPyP: 4'-Methyl-2,2'-bipyridine-4-carbaldehyde (1.00 g, 5.04 mmol) and benzaldehyde (2.14 g, 20.16 mmol) were dissolved in propionic acid (70 mL) and refluxed gently (140 – 150 ^{o}C) for 10 minutes. Pyrrole (1.60 μL, 23.18 mmol) was added to the reaction mixture, which was refluxed in air for 4 hours, whilst covering with aluminum foil. Acid was removed by distillation and porphyrin mixture was re-crystallised from MeOH and stored in fridge overnight. Supernatant liquid was discarded and remaining black residue was dissolved in a minimum amount of DCM and purified by silica gel column using pure DCM and several drops of MeOH. Fractions were monitored by TLC (20:1 DCM: MeOH) and desired spot was

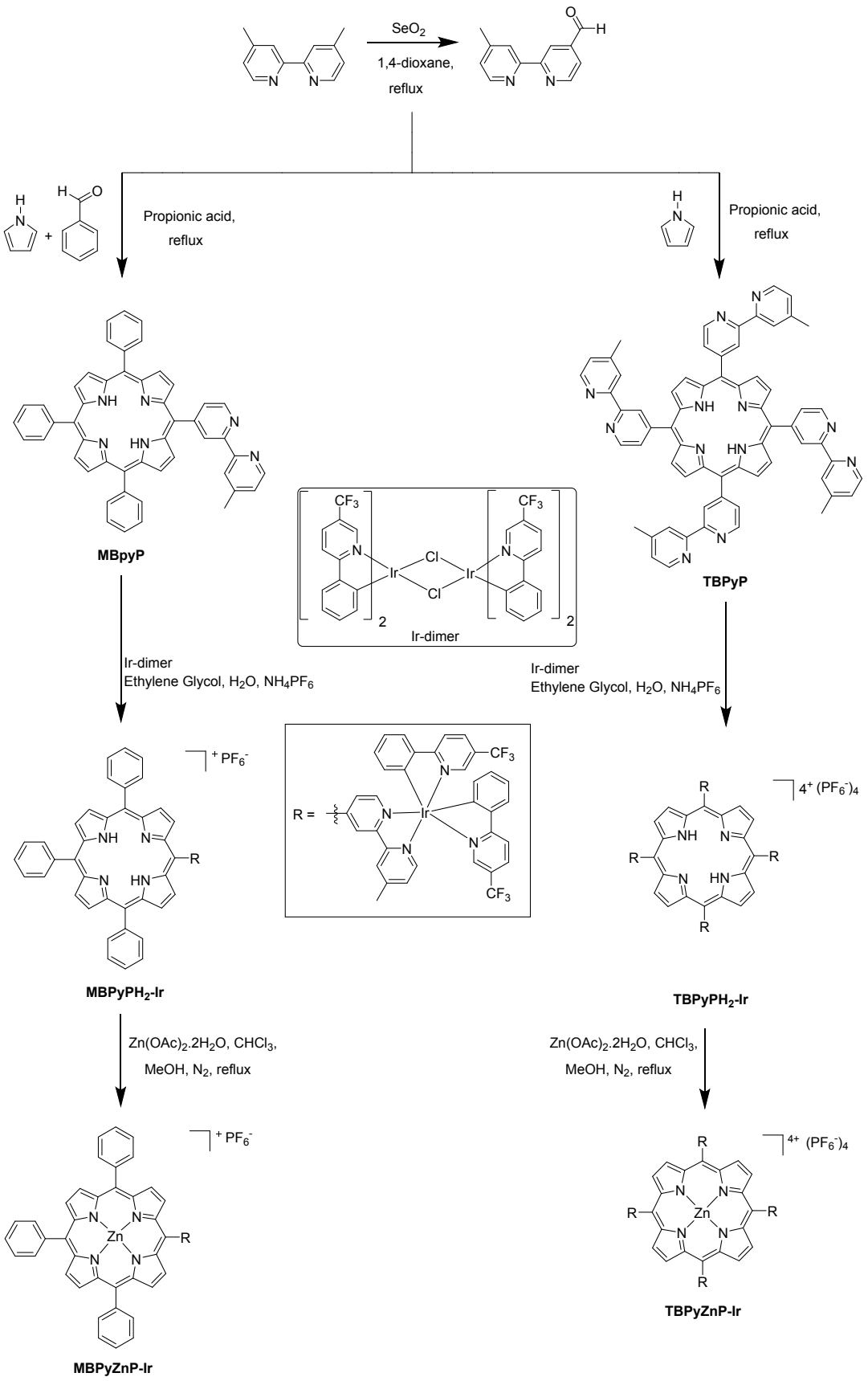

Scheme S1. Synthesis of **MBPyZnP-Ir** and **TBPyZnP-Ir**.

collected, concentrated by rotary evaporation and vacuum dried to afford **MBPyP** (182.60 mg, 0.26 mmol, 5.13 % yield) as a dark reddish solid. ^{1}H NMR (400 MHz, $CDCl_3$, δ ppm): 9.23 (s, 1H), 9.01–9.00 (d, *J* = 4 Hz, 1H), 8.80–8.79 (d, *J* = 4 Hz, 7H), 8.45 (s, 1H), 8.44–8.42 (d, *J* = 8 Hz, 1H), 8.15–8.13 (dd, *J* = 8 Hz, *J* = 8 Hz, 6H), 8.10–8.09 (dd, *J* = 4 Hz, *J* = 4 Hz, 1H), 7.80–7.78 (m, 1H), 7.70–7.67 (m, 8H), 7.62–7.60 (m, 1H), 7.11–7.10 (d, *J* = 4 Hz, 1H), 2.47 (s, 3H), –2.86 (s, 2H). ^{13}C NMR (101 MHz, $CDCl_3$, δ ppm): 155.92, 154.83, 151.51, 149.25, 148.35, 147.50, 142.07, 142.01, 139.19, 134.60, 133.91, 132.24, 131.21, 130.12, 129.52, 128.93, 128.43, 128.09, 127.82, 126.96, 126.74, 124.99, 122.60, 120.84, 120.51, 116.74, 29.73, 21.34 (Fig S11). MALDI - TOF: $C_{49}H_{34}N_6$, 707.2917 (Calcd M^+), 707.0474 (Found M^+).

MBPyPH_2-Ir: MBPyP (40.0 mg, 0.057 mmol) and bis(2-phenyl-5-(trifluorophenyl)-pyridine) iridium (III) dichloro-bridged dimer (38.3 mg, 0.029 mmol) were dissolved in a 1:1 mixture of ethylene glycol and water (20 mL each) and the mixture was refluxed in air overnight. Reaction mixture was cooled to room temperature and transferred into a beaker containing ice. NH_4PF_6 (aq) (15 mL) was added to mixture which was then stirred for 2 hours. Mixture was extracted using DCM and lower organic layer was collected and dried using anhydrous $MgSO_4$; $MgSO_4$ was added to mixture and stirred for 1 hour before collecting supernatant liquid by suction filtration. Dried organic layer was collected and concentrated to afford a dark red residue, before re-dissolving in DCM and purifying by silica gel column using 8:1 DCM: acetone. Fractions were monitored by TLC (using same system as column) and desired spot was collected, concentrated by rotary evaporation and vacuum dried to afford **MBPyPH_2-Ir** (44.0 mg, 0.03 mmol, 51.9 % yield) as a dark red purplish solid. ^{1}H NMR (400 MHz, acetone-D_6, δ ppm): 9.73 (s, 1H), 9.06–8.89 (m, 7H), 8.67–8.60 (m, 5H), 8.50–8.42 (m, 4H), 8.27–8.22 (m, 7H), 8.18–8.13 (m, 3H), 7.90–7.84 (m, 8H), 7.78–7.75 (m, 1H), 7.69–7.67 (d, *J* = 4 Hz, 1H), 7.19–7.15 (m, 2H), 7.12–7.08 (m, 2H), 6.65–6.63 (m, 1H), 6.54–6.52

(m, 1H), 2.52 (s, 3H), –2.78 (s, 2H). ^{13}C NMR spectrum could not be obtained for **MBPyH$_2$-Ir**. MALDI - TOF: $C_{73}H_{48}F_6IrN_8$, 1343.3536 (Calcd $[M–PF_6]^+$), 1343.3587 (Found $[M–PF_6]^+$).

MBPyZnP-Ir: MBPyPH$_2$-Ir (15.8 mg, 0.011 mmol) was dissolved in $CHCl_3$ (30 mL) and $Zn(OAc)_2.2H_2O$ (23.3 mg, 0.11 mmol) was dissolved in MeOH (4 mL) and both were mixed; the reaction mixture was stirred at 60 ^{o}C under N_2 overnight. After cooling to room temperature, the reaction mixture was concentrated, re-dissolved in $CHCl_3$ (40 mL) and washed with H_2O (70 mL); organic layer was collected and dried by adding sodium sulphate and stirring for 1 hour. Mixture was filtered and concentrated to afford a dark green solid, before re-dissolving in $CHCl_3$ and purifying by silica gel column using pure $CHCl_3$. Fractions were monitored by TLC (using pure DCM) and desired spot was collected, concentrated by rotary evaporation and vacuum dried to afford **MBPyZnP-Ir** (13.4 mg, 0.0090 mmol, 81.5 % yield) as a dark green crystalline solid. ^{1}H NMR (400 MHz, acetone-D_6, δ ppm): 10.07 (s, 1H), 9.47–9.29 (m, 8H), 9.08–8.89 (m, 8H), 8.65–8.57 (m, 10H), 8.24 (s, 9H), 8.09 (s, 1H), 7.59–7.52 (m, 4H), 7.07–6.97 (m, 2H), 2.95 (s, 3H). ^{13}C NMR spectrum could not be obtained for **MBPyZnP-Ir**. MALDI - TOF: $C_{73}H_{46}F_6IrN_8Zn$, 1405.2657 (Calcd $[M–PF_6]^+$), 1405.0349 (Found $[M–PF_6]^+$).

MBPyZnP: MBPyZnP was synthesized by the same procedure as described above for **MBPyZnP-Ir**, except using **MBPyP** instead of **MBPyPH$_2$-Ir**. **MBPyZnP** (15.6 mg, 0.02 mmol, 70.1 % yield) was afforded as a dark purple crystalline solid. ^{1}H and ^{13}C NMR spectra could not be obtained for **MBPyZnP**. MALDI - TOF: $C_{49}H_{32}N_6Zn$, 768.1974 (Calcd M^+), 768.1932 (Found M^+).

TBPyP: 4’-Methyl-2,2’-bipyridine-4-carbaldehyde (208.8 mg, 1.050 mmol) was dissolved in propionic acid (70 mL) and refluxed gently (140 - 150 ^{o}C) for 10 minutes. Pyrrole (77 μL, 1.11 mmol) was added to reaction mixture and refluxed in air for 4 hours, whilst covering

with aluminum foil. Propionic acid was removed by flushing with air overnight. Remaining black precipitate was completely dissolved in $CHCl_3$ and purified by silica gel column using pure $CHCl_3$ and a few drops of MeOH. Fractions were monitored by TLC (10:1 DCM: MeOH) and desired spot was collected, concentrated by rotary evaporation and vacuum dried to afford a black reddish precipitate. Solid was recrystallized from MeOH to afford **TBPyP** (40.0 mg, 0.041 mmol, 3.9 % yield) as a dark reddish solid. ^{1}H NMR (400 MHz, $CDCl_3$, δ ppm): 9.27 (s, 4H), 9.04–9.03 (d, J = 4 Hz, 4H), 8.87 (s, 7H), 8.49–8.44 (m, 9H), 8.11–8.10 (d, J = 4 Hz, 4H), 7.13 (s, 4H), 2.48 (s, 12H), –2.91 (s, 2H). ^{13}C NMR (101 MHz, $CDCl_3$, δ ppm): 155.80, 155.02, 150.95, 149.30, 148.32, 147.60, 129.47, 126.91, 125.04, 122.57, 118.08, 21.33 (Fig S15). MALDI - TOF: $C_{46}H_{46}N_{12}$, 983.4041 (Calcd M^+), 983.2643 (Found M^+).

TBPyPH$_2$-Ir: TBPyPH$_2$-Ir was synthesized by the same procedure as described above for **MBPyPH$_2$-Ir**, except using **TBPyP** instead of **MBPyP**. **TBPyPH$_2$-Ir** (64.8 mg, 0.016 mmol, 43.8 % yield) was isolated as a dark red purplish solid. ^{1}H NMR (400 MHz, acetonde-D_6, δ ppm): 9.67 (s, 4H), 9.30–8.46 (m, 40H), 8.25–8.13 (m, 16H), 7.68 (s, 4H), 7.21–7.09 (m, 16H), 6.65–6.53 (m, 8H), 2.52 (s, 12H), –2.91 (s, 2H). ^{13}C NMR could not be obtained for TBPyPH$_2$-Ir. MALDI - TOF: $C_{160}H_{102}F_{24}Ir_4N_{20}$, 3964.5671 (Calcd $[M–PF_6]^+$), 3964.5739 (Found $[M–PF_6]^+$).

TBPyZnP-Ir: TBPyZnP-Ir was synthesized by the same procedure as for **MBPyZnP-Ir**, except using **TBPyPH$_2$-Ir** instead of **MBPyPH$_2$-Ir**. **TBPyZnP-Ir** (23.1 mg, 0.0055 mmol, 80.0 % yield) was obtained as a dark green crystalline solid. ^{1}H NMR (400 MHz, acetone-D_6, δ ppm): 9.92–9.77 (m, 4H), 9.19–8.50 (m, 40H), 8.26–8.14 (m, 16H), 7.70 (s, 4H), 7.21–7.20, 7.14–7.13 (m, 16H), 6.67–6.57 (m, 8H), 2.56–2.54 (d, J = 8 Hz, 12H). ^{13}C NMR could not be obtained for **TBPyZnP-Ir**. MALDI - TOF: $C_{160}H_{100}F_{24}Ir_4N_{20}Zn$, 4027.4786 (Calcd $[M–PF_6]^+$), 4027.4762 (Found $[M–PF_6]^+$).

TBPyZnP: TBPyZnP was synthesized by the same procedure as for **MBPyZnP-Ir**, except using **TBPyP** instead of **MBPyP-Ir**. **TBPyZnP** (25.3 mg, 0.024 mmol, 78.0 % yield) was afforded as a dark purple crystalline solid. ^{1}H and ^{13}C NMR could not be obtained for **TBPyZnP**. MALDI - TOF: $C_{64}H_{44}N_{12}Zn$, 1044.3098 (Calcd M^{+}), 1044.3086 (Found M^{+}) (Fig S23).

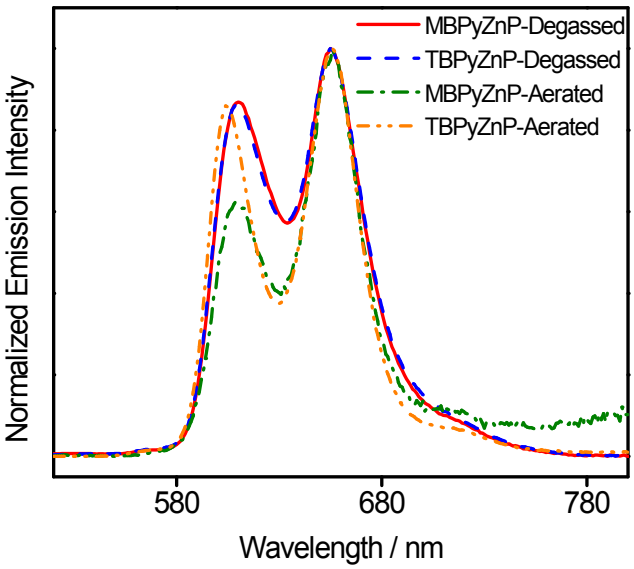

Fig S1. Normalized emission spectra of aerated and degassed **MBPyZnP** and **TBPyZnP** in MeCN at room temperature.

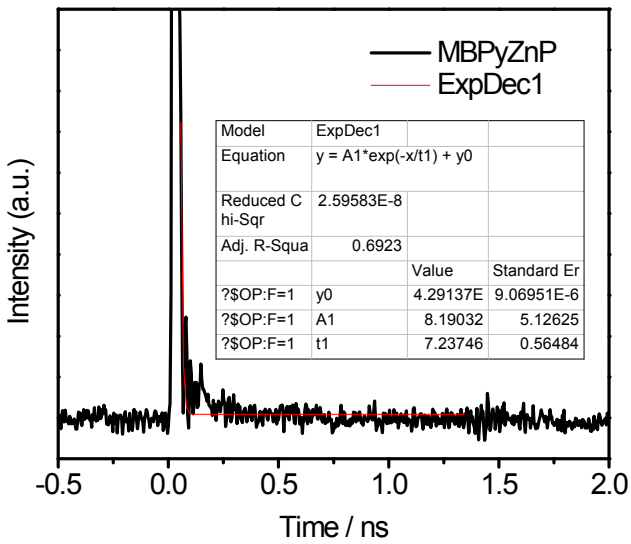

Fig S2. Emission decay profile for **MBPyZnP** in aerated MeCN monitored at 610 nm.

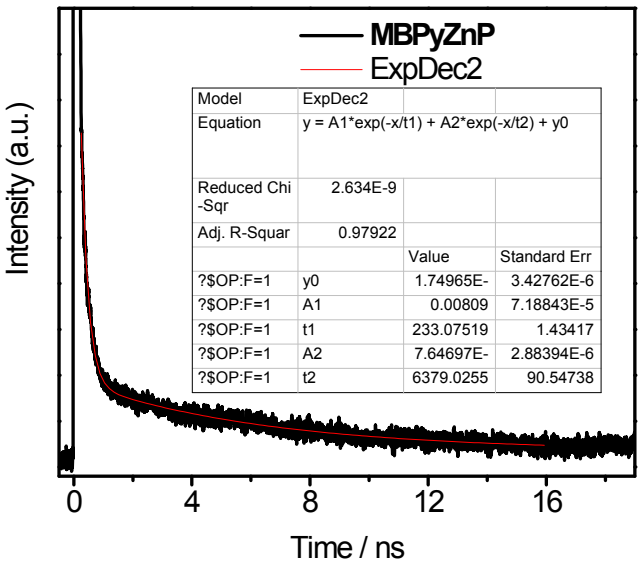

Fig S3. Emission decay profile for **MBPyZnP** in degassed MeCN monitored at 610 nm.

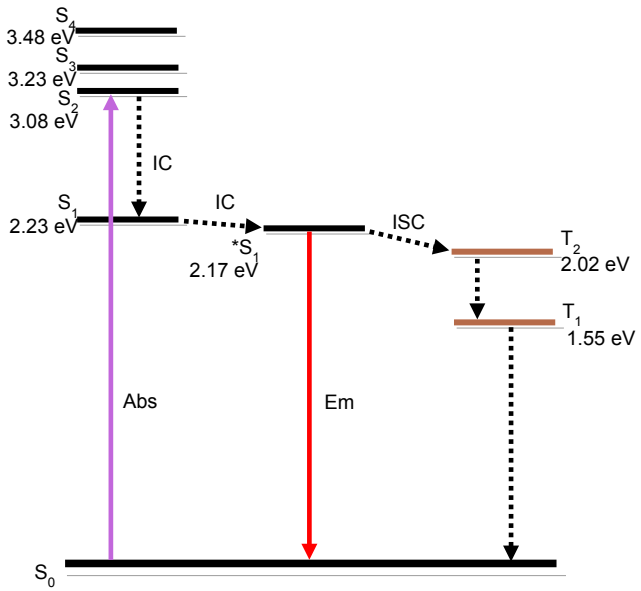

Fig S4. Jablonski energy diagram of **MBPyZnP** based on the computation at B3LYP/GENECP/LANL2DZ level in acetonitrile.

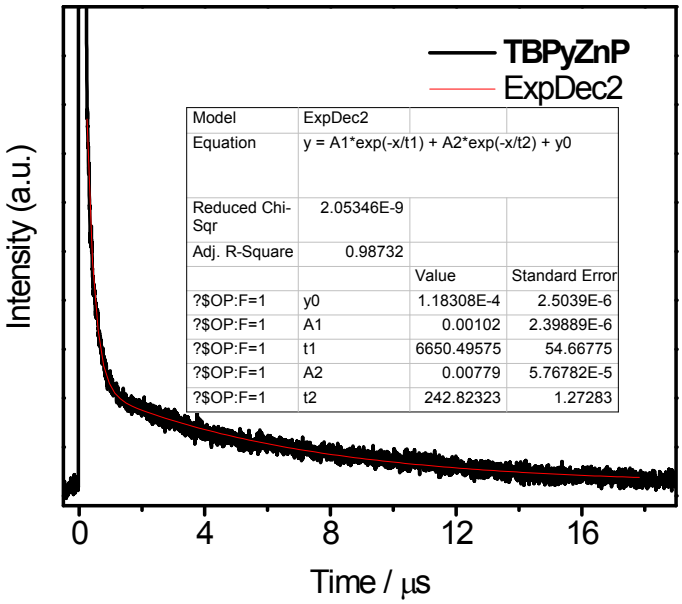

Fig S5. Emission decay profile for **TBPyZnP** in degassed MeCN monitored at 610 nm.

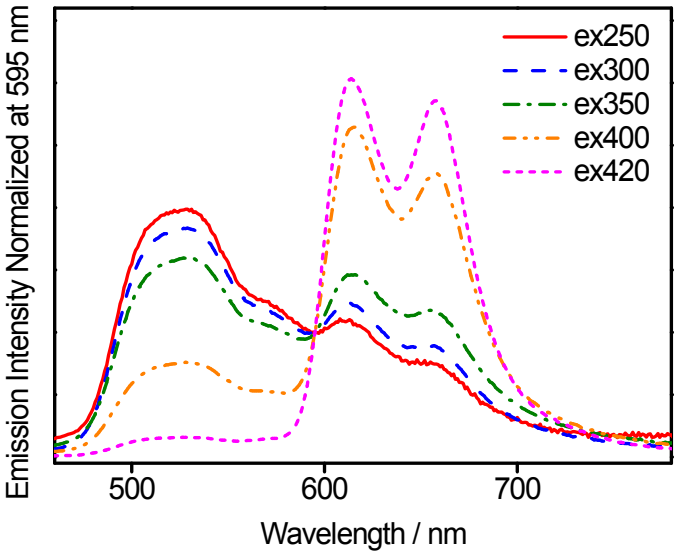

Fig S6. Emission spectra of **MBPyZnP-Ir** normalized at 595 nm at different excitation wavelength in MeCN at room temperature.

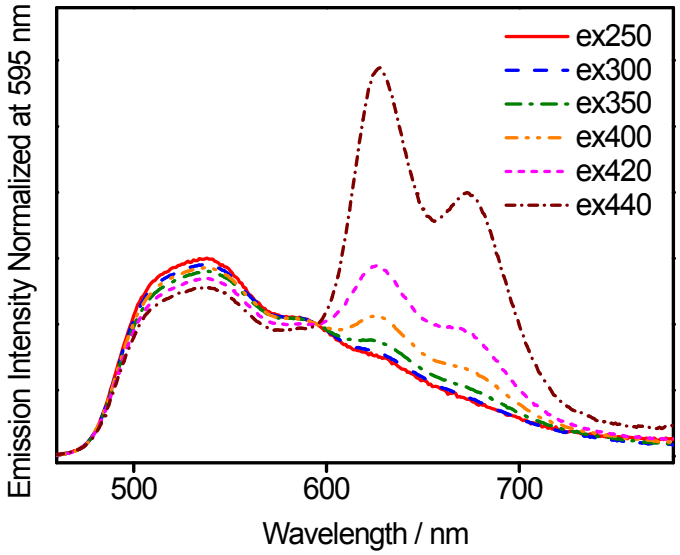

Fig S7. Emission spectra of **TBPyZnP-Ir** normalized at 595 nm at different excitation wavelength in MeCN at room temperature.

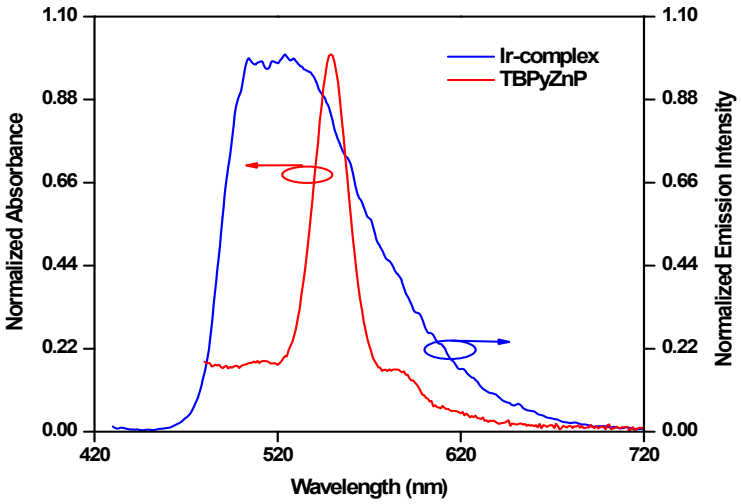

Fig S8. Spectral overlap of the normalized fluorescence spectrum of Ir-complex excited at 430-455 nm with the normalized absorption spectrum of **TBPyZnP**.

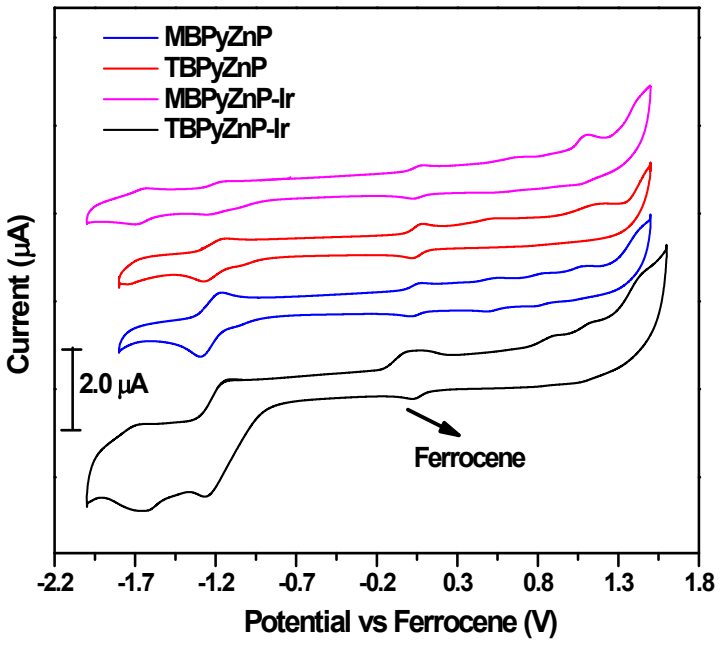

Fig S9. Cyclic voltammograms of the porphyrins recorded in MeCN (100 μM) at room temperature.

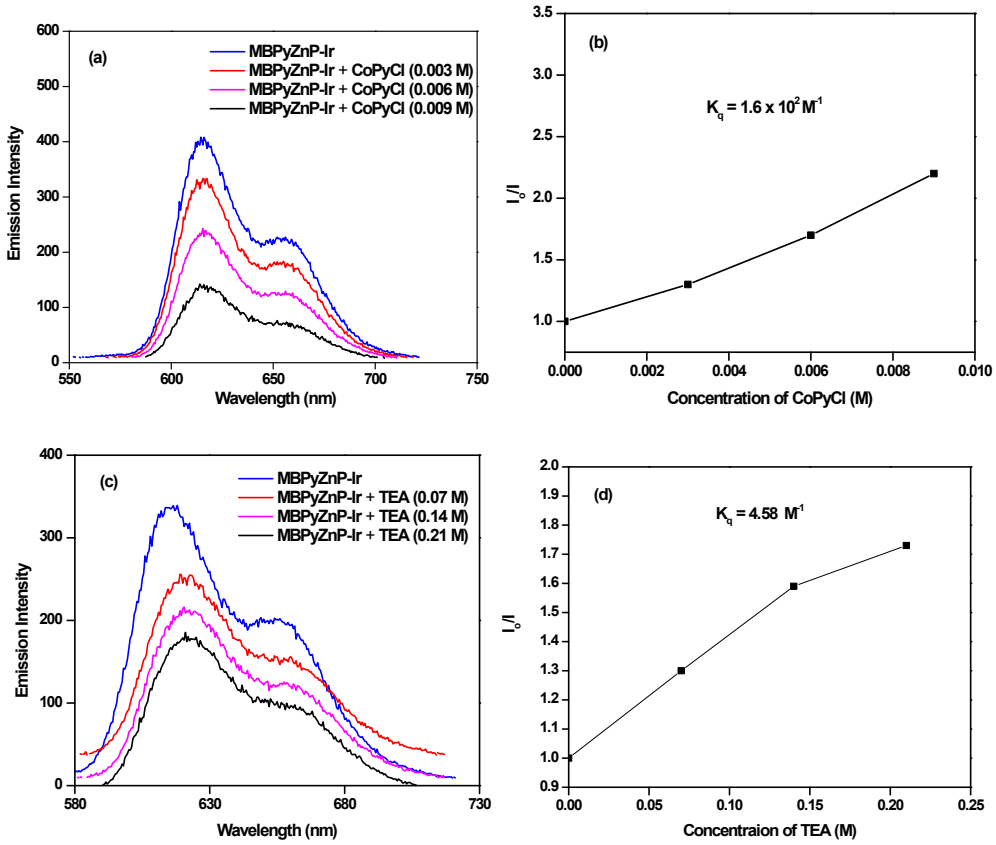

Fig S10. Phosphorescence quenching of **MBPyZnP-Ir** (10 μM) with (a) **CoPyCl** and (c) TEA as quencher in MeCN; Stern-Volmer plot of **MBPyZnP-Ir** with (b) **CoPyCl** and (d) TEA as quencher.

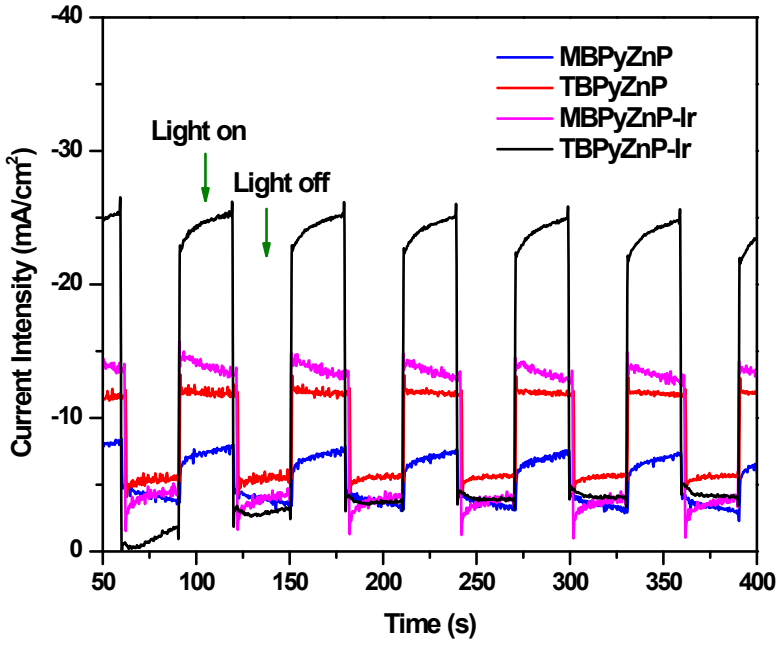

Fig S11. Photocurrent response of the porphyrins.

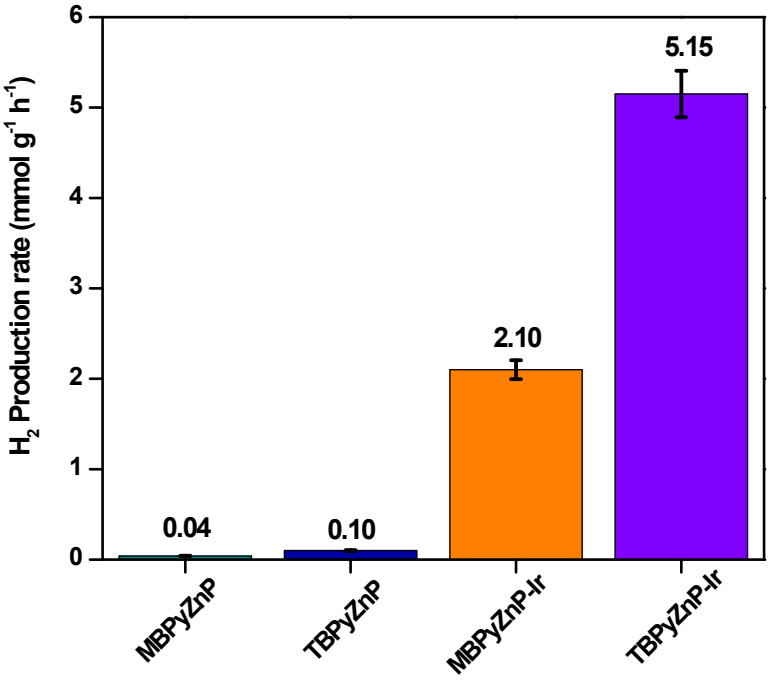

Fig S12. H_2 production rate of PSs (Photosensitizer (0.1 mM) + TEA (0.8 M) + **CoPyCl** (0.4 mM) + MeCN/H_2O (1:2 v/v)) under irradiation for 5 h.

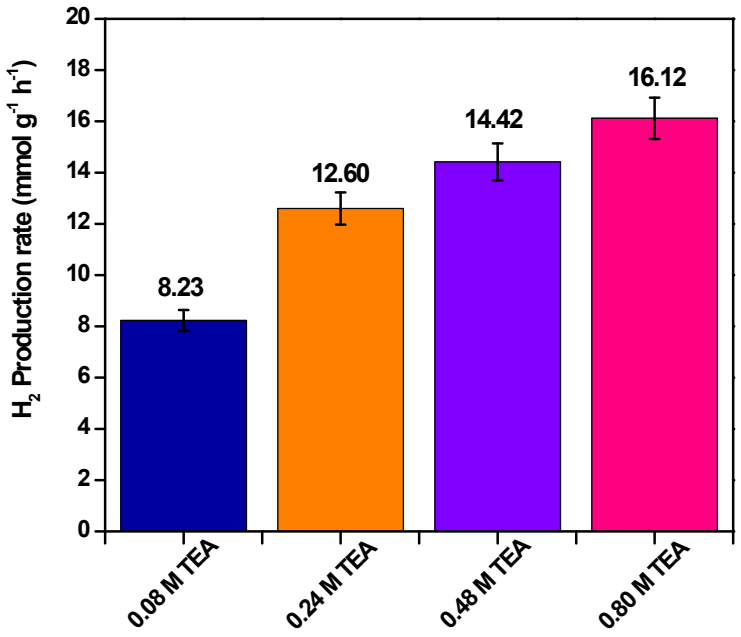

Fig S13. H_2 production rate of PSs (**TBPyZnP-Ir** (0.1 mM) + TEA (0.08–0.8 M) + **CoPyCl** (0.4 mM) + MeCN/H_2O (2:1 = v/v)) under irradiation for 5 h.

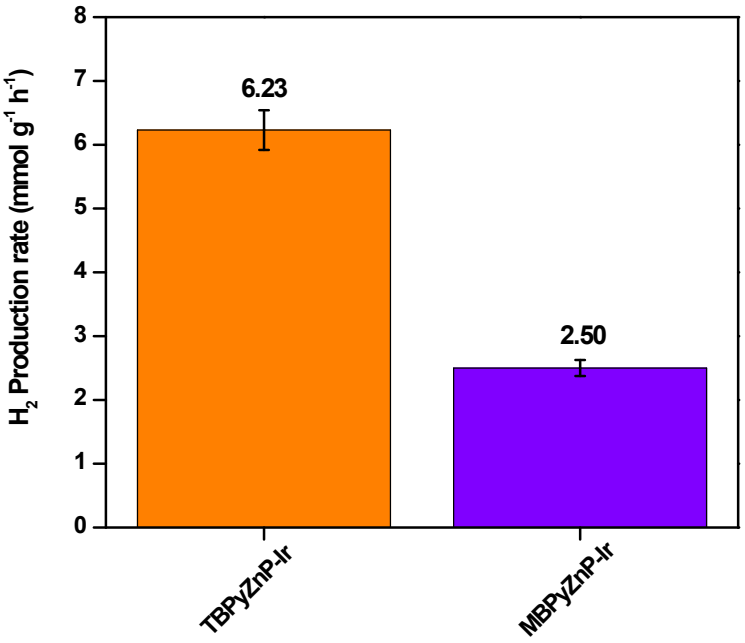

Fig S14. H_2 production rate of PSs (Photosensitizer (0.1 mM) + TEA (0.8 M) + **CoPyCl** (0.2 mM) + MeCN/H_2O (2:1 = v/v)) under irradiation for 5 h.

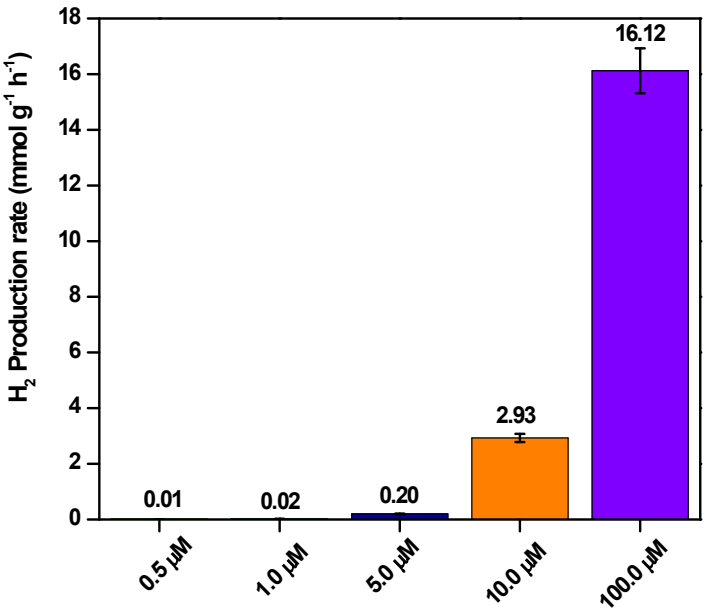

Fig S15. H_2 production rate of PSs (**TBPyZnP-Ir** (0.5 -100 μM) + TEA (0.8 M) + **CoPyCl** (0.4 mM) + MeCN/H_2O (2:1 = v/v)) under irradiation for 5 h.

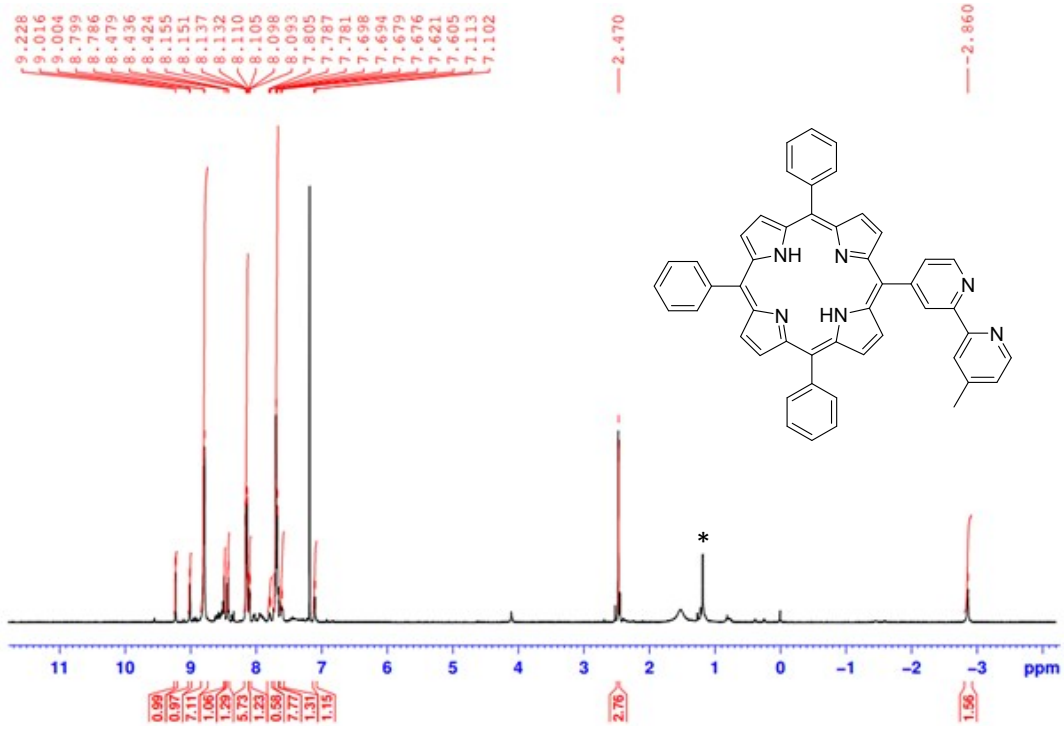

Fig S16. ^1H NMR spectrum of **MBPyP** recorded in $CDCl_3$.

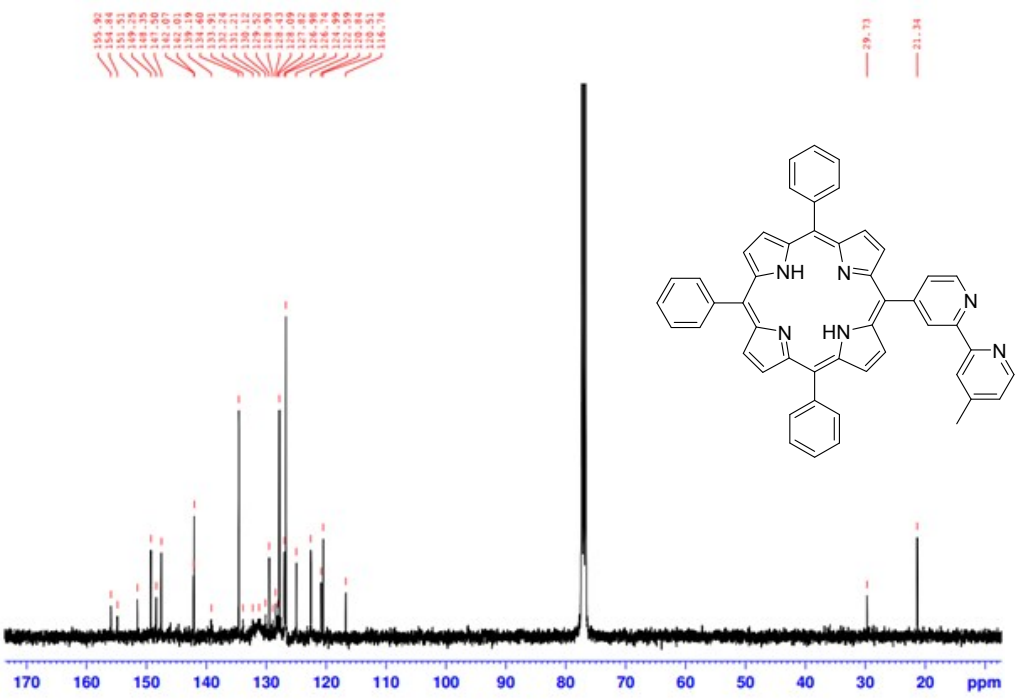

Fig S17. ^{13}C NMR spectrum of **MBPyP** recorded in $CDCl_3$.

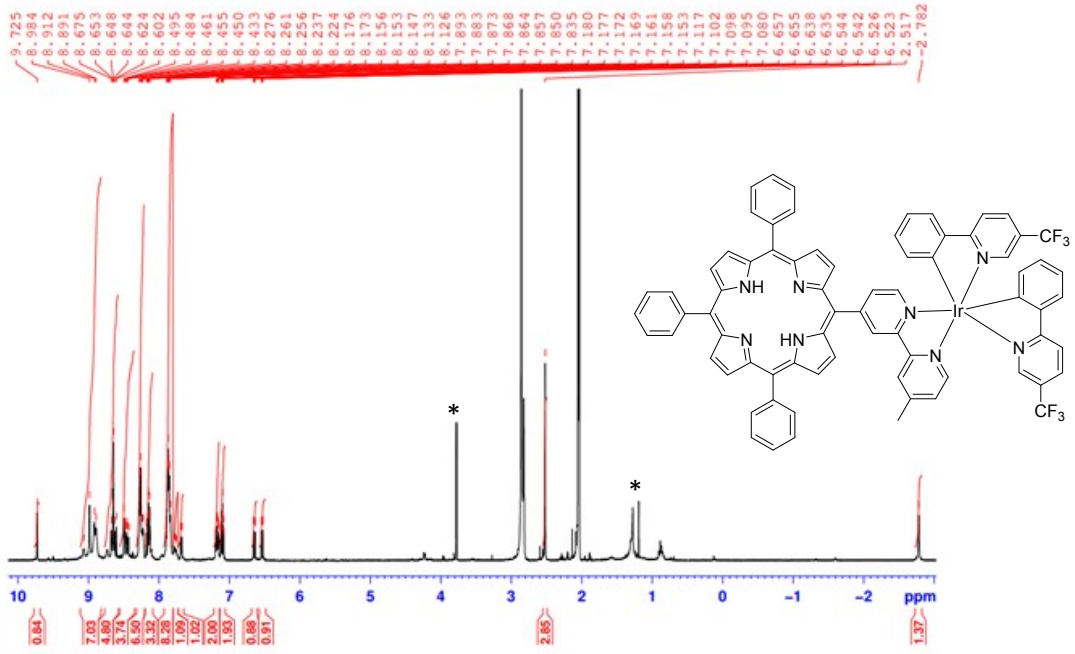

Fig S18. ^{1}H NMR spectrum of **MBPyPH$_2$-Ir** recorded in acetone-D_6. ^{13}C NMR spectrum could not be obtained for **MBPyP-Ir**.

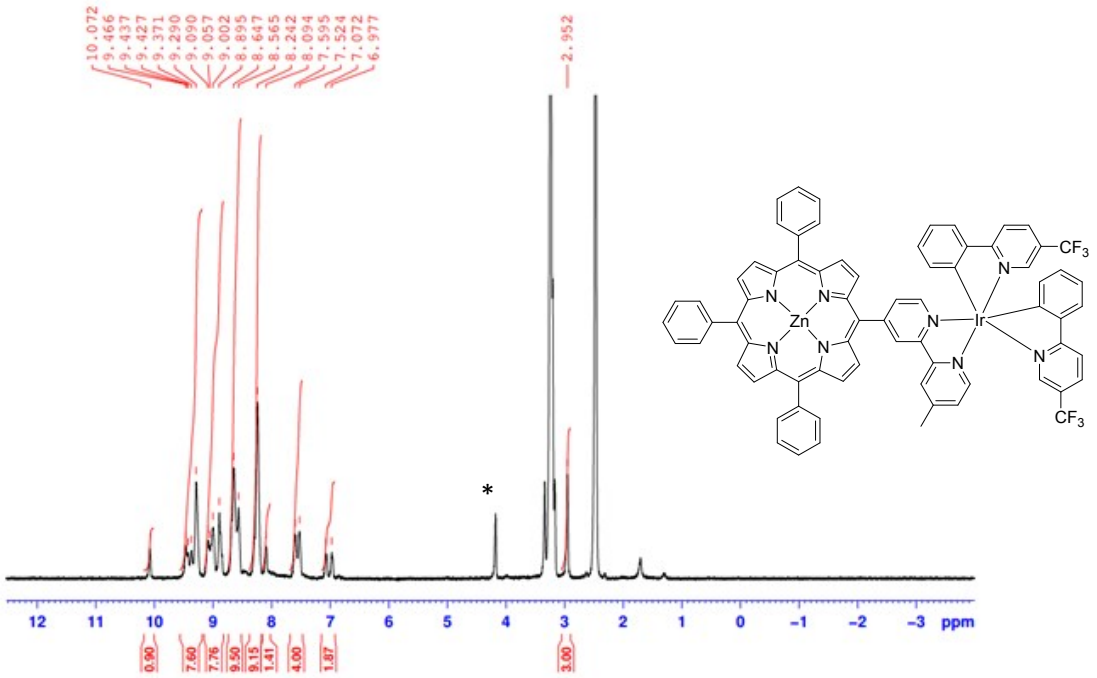

Fig S19. ^{1}H NMR spectrum of **MBPyZnP-Ir** recorded in acetone-D_6. ^{13}C NMR spectrum could not be obtained for MBPyZnP-Ir.

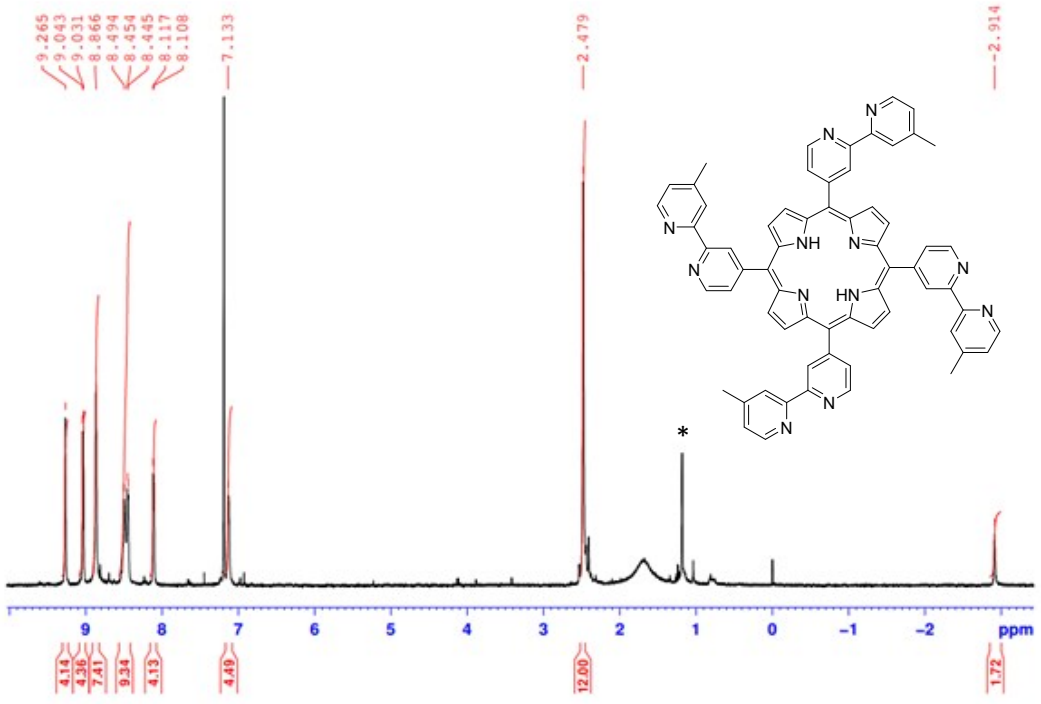

Fig S20. ^{1}H NMR spectrum of **TBPyP** recorded in $CDCl_3$.

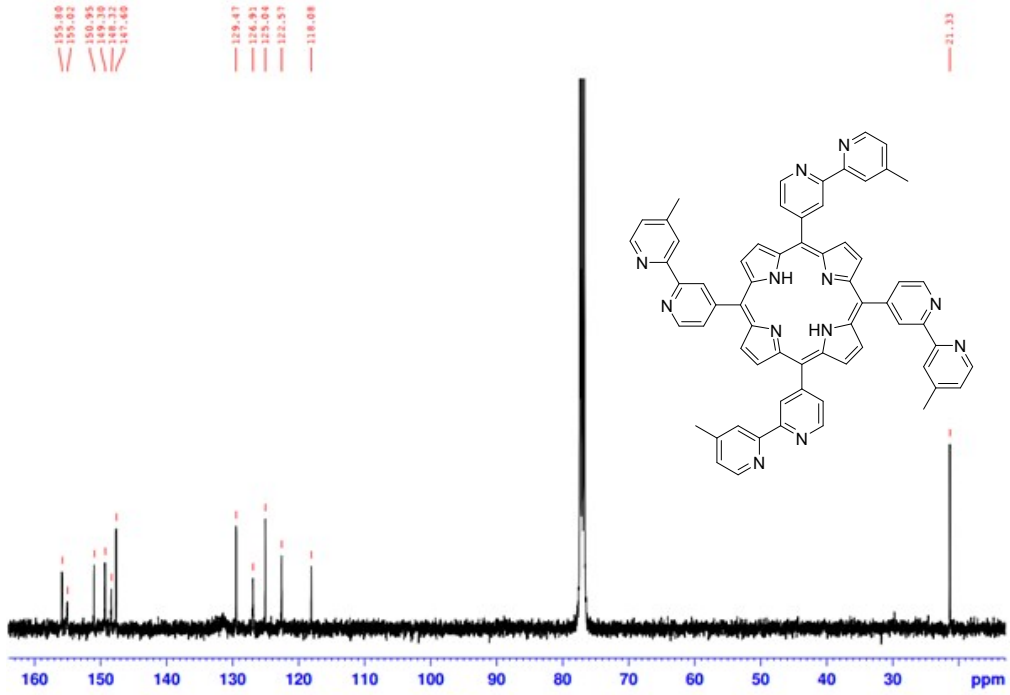

Fig S21. ^{13}C NMR spectrum of **TBPyP** recorded in $CDCl_3$.

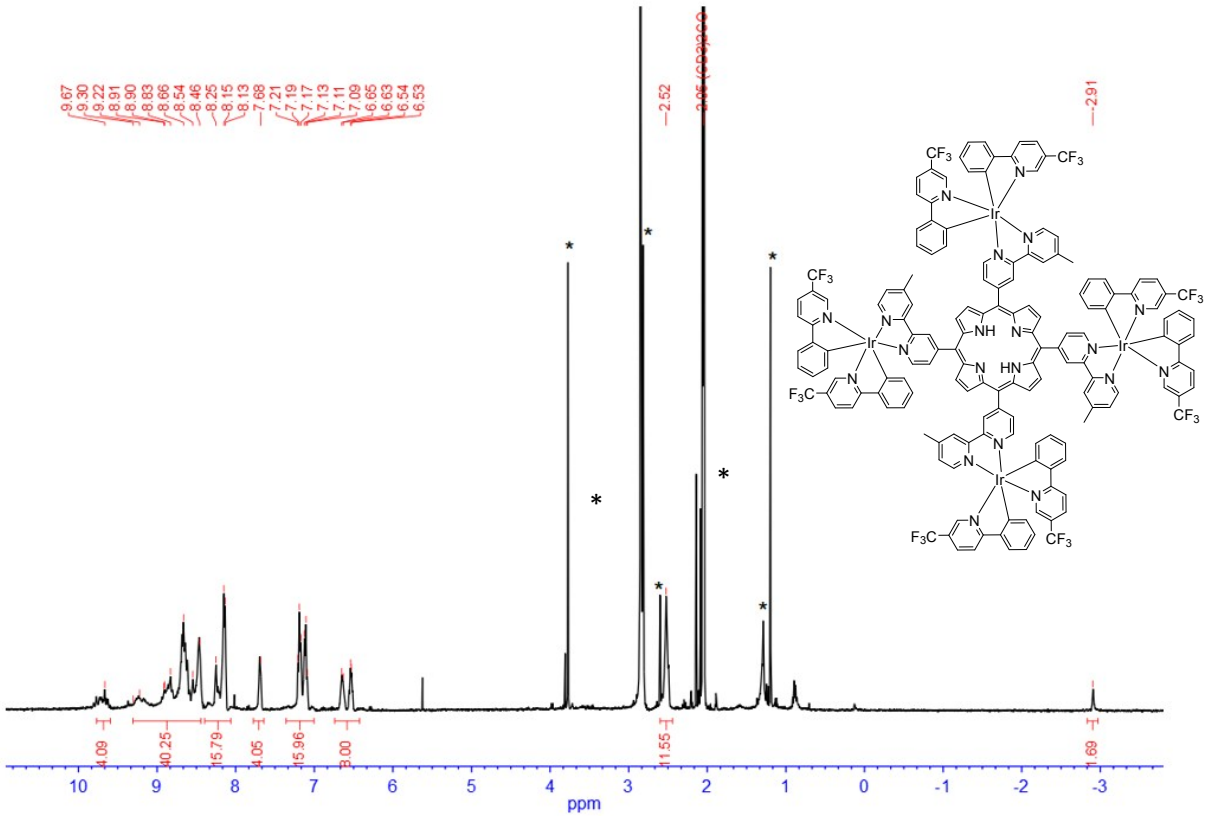

Fig S22. ^{1}H NMR spectrum of **TBPyPH$_2$-Ir** recorded in acetone-D_6. ^{13}C NMR spectrum could not be obtained for **TBPyPH$_2$-Ir**.

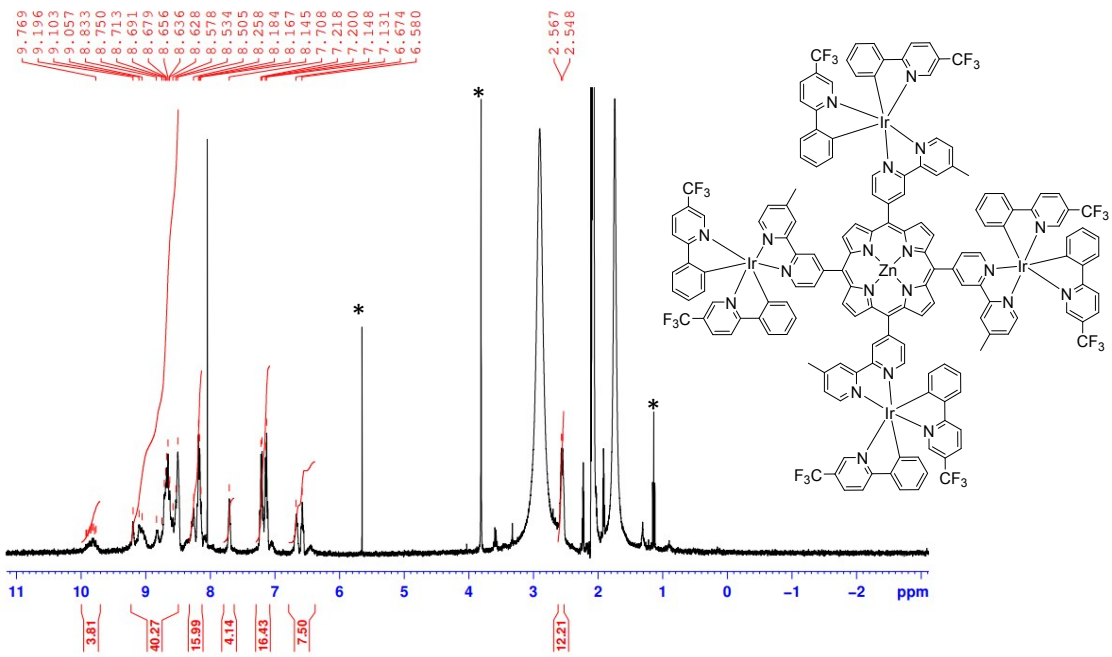

Fig S23. ^{1}H NMR spectrum of **TBPyZnP-Ir** recorded in acetone-D_6. ^{13}C NMR spectrum could not be obtained for **TBPyZnP-Ir**.

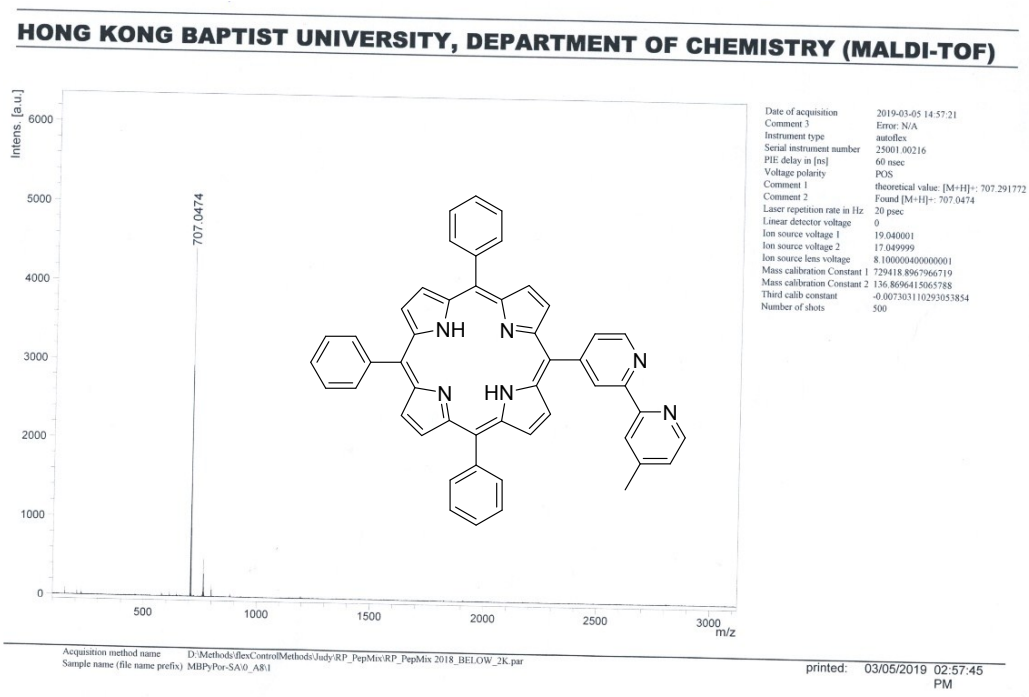

Fig S24. MALDI-TOF MS spectrum of **MBPyP**.

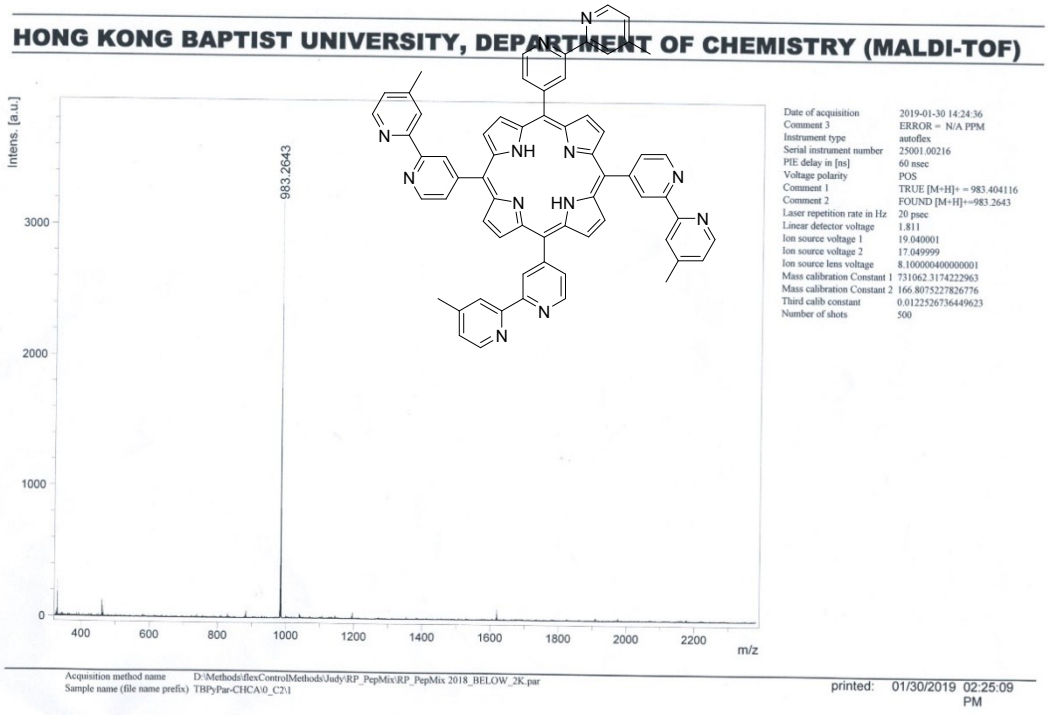

Fig S25. MALDI-TOF MS spectrum of **TBPyP**.

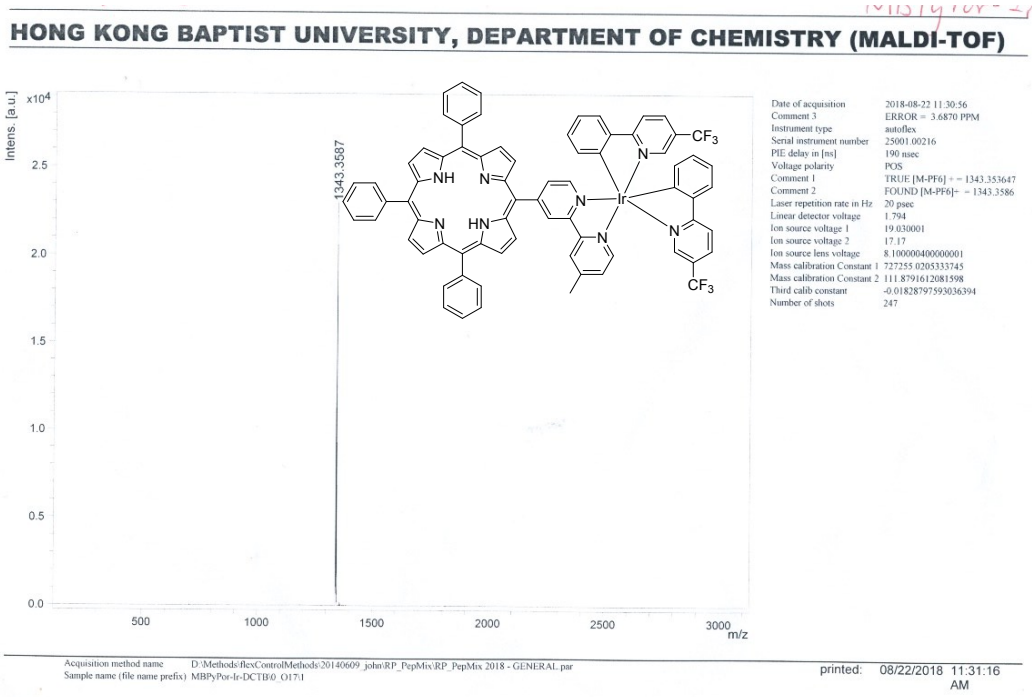

Fig S26. MALDI-TOF MS spectrum of **MBPyPH$_2$-Ir**.

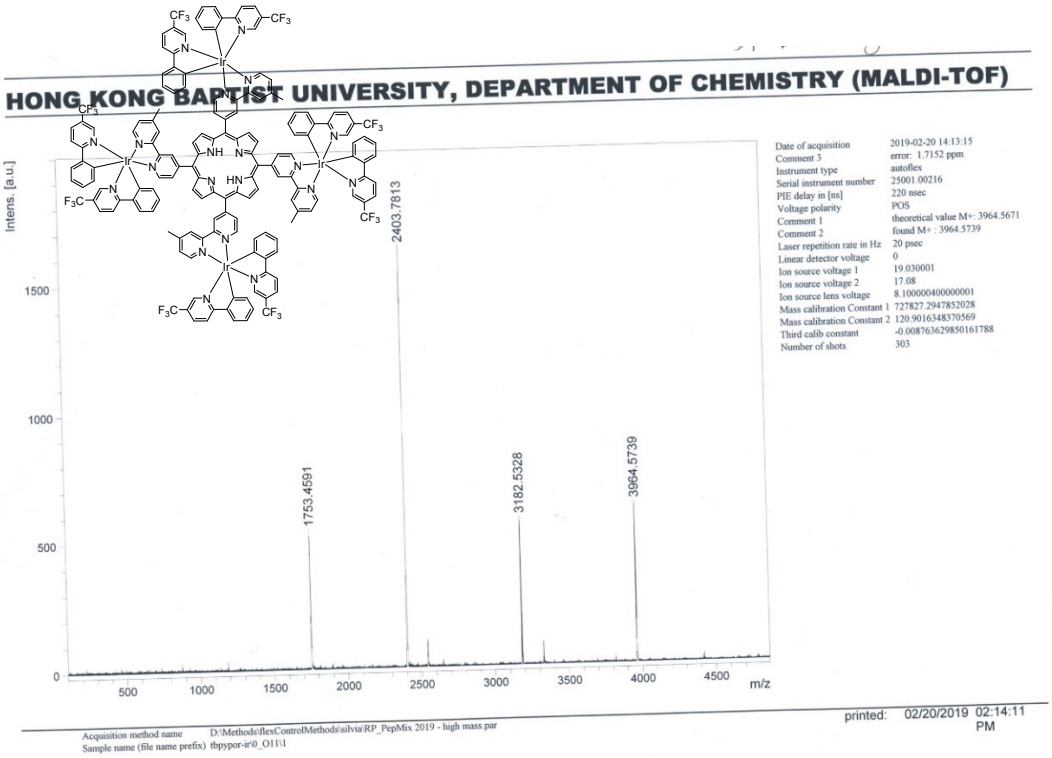

Fig S27. MALDI-TOF MS spectrum of **TBPyPH$_2$-Ir**.

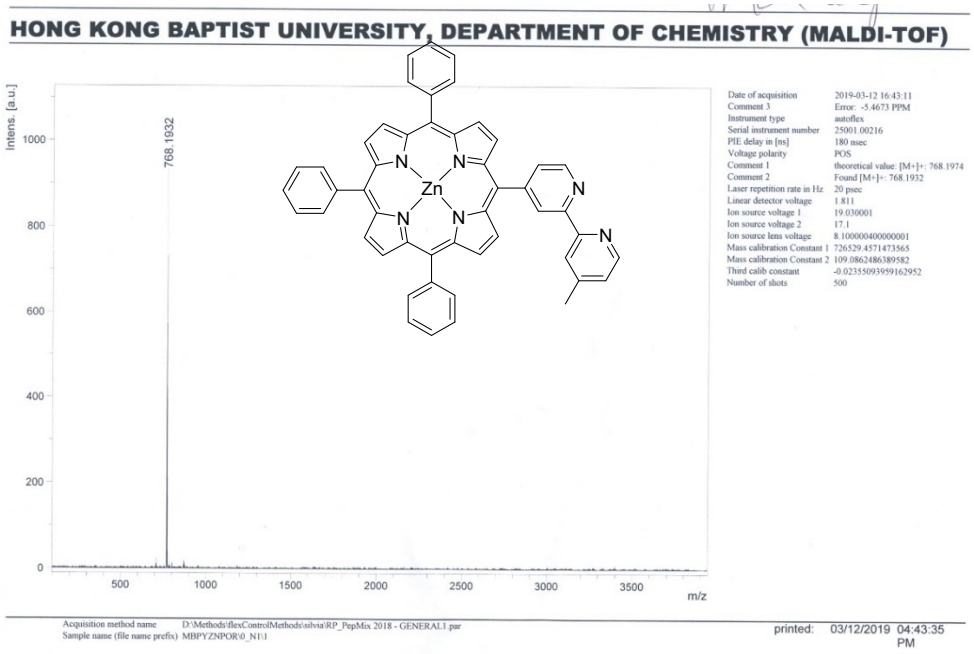

Fig S28. MALDI-TOF MS spectrum of **MBPyZnP**.

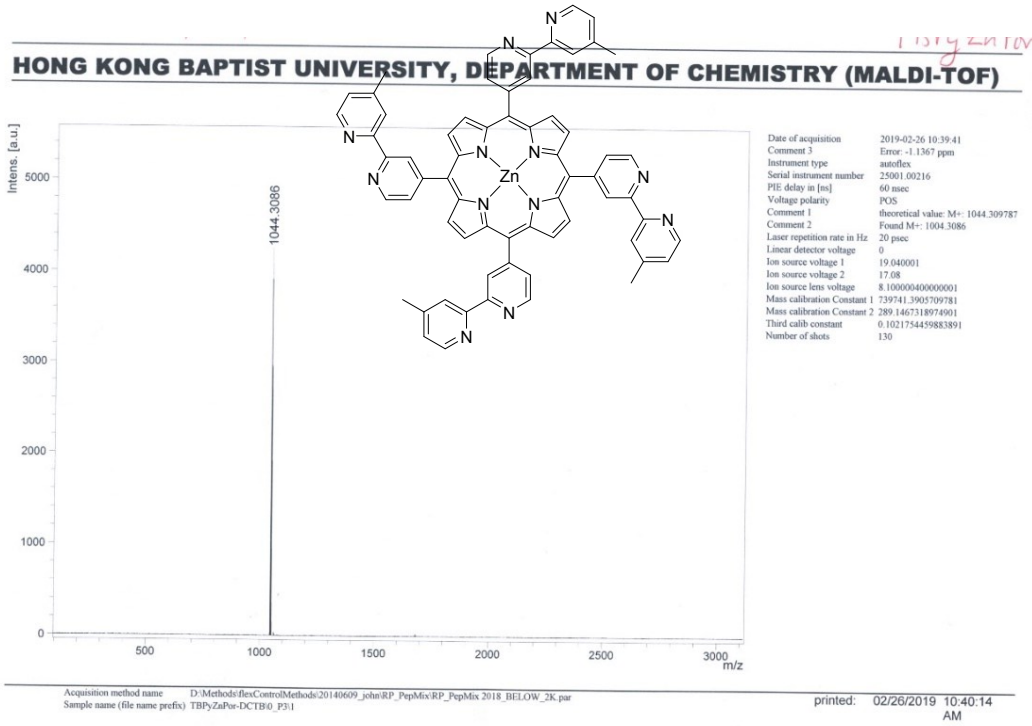

Fig S29. MALDI-TOF MS spectrum of **TBPyZnP**.

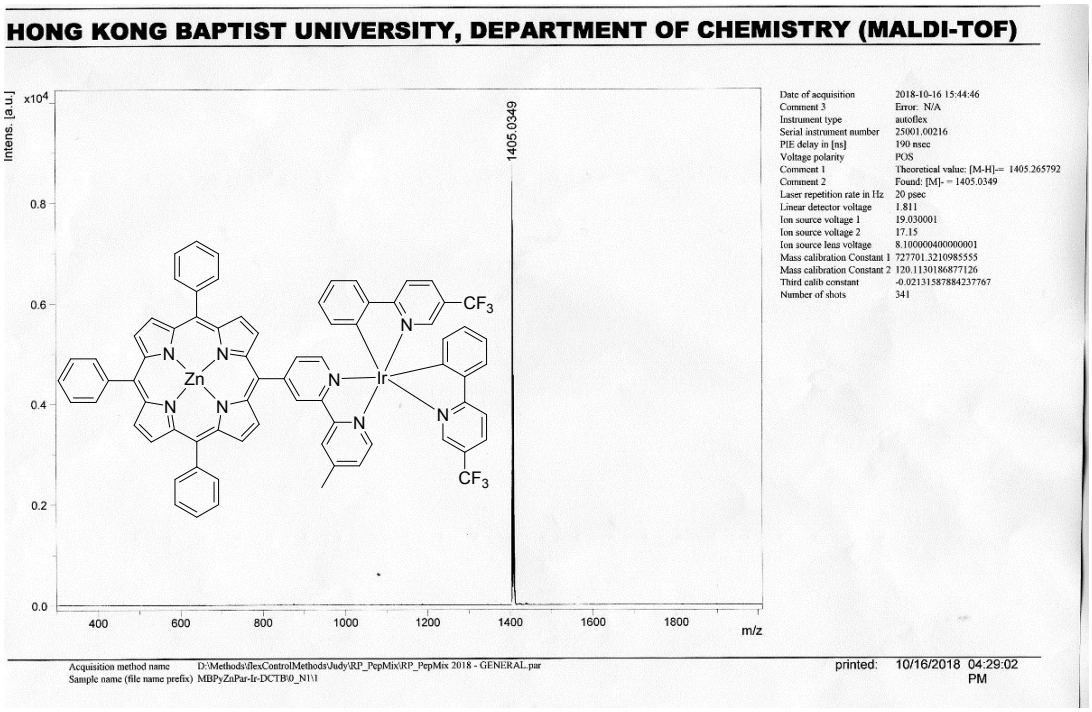

Fig S30. MALDI-TOF MS spectrum of **MBPyZnP-Ir**.

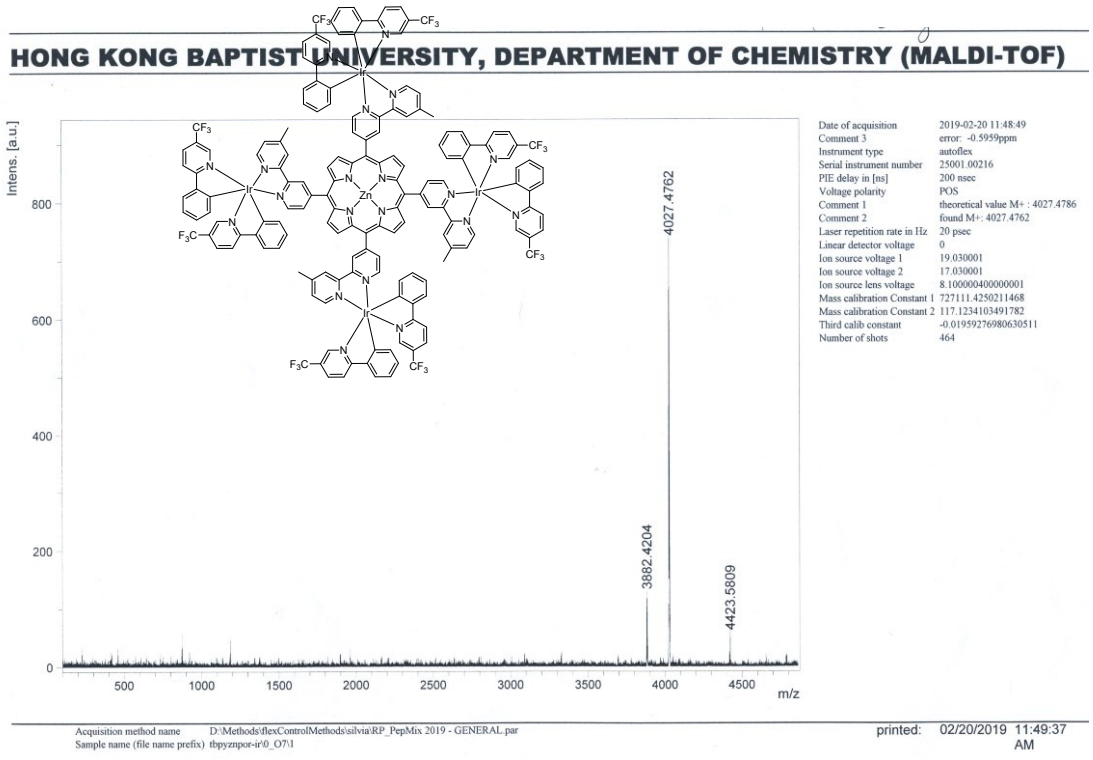

Fig S31. MALDI-TOF MS spectrum of **TBPyZnP-Ir**.

References:

(1) J. N. Demas and G. A. Crosby, *J. Phys. Chem.,* 1971, **75**, 991-1024.

(2) K. Nakamaru, *Bull. Chem. Soc. Jpn.,* 1982, **55**, 1639-1640.

(3) K. Araki, P. Losco, F. M. Engelmann, H. Winnischofer and H. E. Toma, *J. Photochem. Photobiol. A,* 2001, **142**, 25-30.

(4) D. Wang, H.-G. Chen, X.-C. Tian, X.-X. Liang, F.-Z. Chen and F. Gao, *RSC Adv.,* 2015, **5**, 107119-107122.

(5) S. Chen, G. Tan, W.-Y. Wong and H.-S. Kwok, *Adv. Funct. Mater.,* 2011, **21**, 3785-3793.